- Technical Paper -

STUDY ON CARBONATION PROGRESS IN HARDENED CEMENT PASTE ASSOCIATED WITH MOISTURE PENETRATION

Luge CHENG[*1], Naohiko SAEKI [*2], Ryo KURIHARA[*1], Ippei MARUYAMA [*3, *4]

ABSTRACT

Impact of carbonation on moisture penetration and mineralogical profile in cement paste when moisture and CO_2 penetration from one direction was studied under four different RH (23-80%) and T (20 and 40℃) conditions. Results showed increasing RH promotes the carbonation degree of CH while limiting the carbonation process by water blockage. High temperature was found to promote carbonation and moisture penetration though not to the same extent. The opposite effects of carbonation on moisture penetration were discussed by comparing the distance between carbonation and moisture penetration depths.

Keywords: carbonation, moisture, relative humidity, temperature, CH, C-S-H

1. INTRODUCTION

Carbonation of cement-based materials is the reaction between CO_2 and the hydration compounds including portlandite (CH) and C-S-H, generating calcium carbonate precipitation with three polymorphic forms: calcite, aragonite, and vaterite [1]. The carbonation of cementitious material can also yield significant microstructural changes in two opposite ways: pore-clogging by the difference of molar volume between CH and the precipitated calcium carbonate (CC) [2], and the microcracks caused by the decalcification of C-S-H [3]. Relative humidity (RH) is an essential influencing factor of the carbonation process, and it has been reported that the peak of carbonation depth can be reached in the humidity range between 50 and 70% [4][5]. Furthermore, the effect of temperature on carbonation has been reported that the carbonation rate can be accelerated by the increasing temperature for Portland cement-based materials [6][7].

In most research, the RH controlling process was usually conducted before the accelerated carbonation process of samples in laboratory experiments [7][8], which is different from the natural carbonation process that the CO_2 and moisture penetration through the cementitious materials simultaneously. However, little research has been done in understanding the carbonation behavior and moisture penetration at the same time. Therefore, this study aims to identify the influence of carbonation on moisture penetration properties and mineralogical profile in OPC (Ordinary Portland cement) cement paste under different relative humidity and temperature conditions, which makes the understanding of the carbonation behavior of RC structures in realistic conditions more precise and reliable.

2. EXPERIMENT METHODS

2.1 Materials and Mix Proportions

OPC was used throughout the experiment, the chemical composition and physical properties of which are shown in Table 1, while Table 2 shows the mineral composition of OPC. Cement paste was made with a water-to-cement ratio (W/C) of 0.55, the deionized water was kept at 20℃ for one day before mixing. The cement and water were mixed by a planetary mixer (ARE-500, THINKY) with a rotation speed of 1000 rpm. To mix the cement paste homogeneously, part of the water was added to the cement to reach a W/C ratio of 0.30 and was mixed for 1.5 min, then water was added to reach the target W/C ratio of 0.55, then mixed for another 1.5 min. After mixing, 500mL polypropylene bottles filled with

Table 1 Chemical Compositions and physical properties of the Ordinary Portland cement

Density (g/cm^3)	Blaine specific surface area (cm^2/g)	Ig.loss	Chemical compositions (%)									
			CaO	SiO_2	Al_2O_3	Fe_2O_3	MgO	K_2O	Na_2O	SO_3	Cl	SUM
3.16	3270	2.28	64.19	19.86	5.55	2.80	1.41	0.41	0.28	2.70	0.015	97.22

Table 2 Mineral Composition (%) of Ordinary Portland Cement

C3S	C2S	C3A	C4AF	Calcite	Bassanite	Gypsum	Periclase	SUM
56.51	18.27	8.55	7.07	4.43	2.78	1.52	0.85	100.0

*1 Dept. of Architecture, the University of Tokyo, JCI Member
*2 Dept. of Architecture, the University of Tokyo, JCI student Member
*3 Prof., Dept. of Architecture, the University of Tokyo, JCI Member
*4 Prof., Dept. of Environmental Engineering and Architecture, Nagoya University, JCI Member

fresh cement paste was put on a roller (IKA ROLLER 10 digital) with a rotation speed of 60 rpm for 3.5 h to minimize the bleeding and segregation. After confirming the cement paste was creamy, it was poured into molds (20×20×20 mm) and vibrated to remove entrapped air bubbles, then the casting surface was covered with polyethylene wrap and placed at 20℃. The specimens were demolded the following day, sealed, and cured at 20℃ in 56 days for the next step of the study after confirming sufficient hydration of cement.

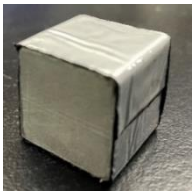

Fig.1 Cement paste sample covered by aluminum adhesive tapes on five surfaces

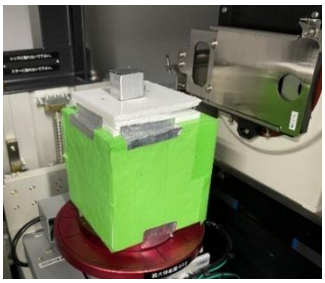

Fig. 2 Setup in x-ray radiography equipment

2.2 Sample Preparation and Exposure

Once cured, the samples were vacuum dried by a freeze dryer (FDM-1000, EYELA) for 48h at 20℃ to remove the evaporable moisture content as the initial state of the samples. After drying, all the specimens were sealed with aluminum adhesive tapes to isolate five surfaces so that only one surface exposed to the controlled environment allowing the CO_2 and moisture penetration can only penetrate from one direction as shown in Fig. 1. These samples were then placed in carbonation incubators containing a 5% concentration of CO_2 at 20℃ with different RHs using saturated salt solutions. (23±5% RH—CH_3CO_2K; 58±5% RH—NaBr, 80±5% RH—water). Besides, a different temperature of 40℃ was used at the 58%±5% RH carbonation to evaluate the effect of temperature.

The samples under each carbonation condition were taken out periodically to monitor the moisture penetration depth by X-ray computed radiography. After 28 days of carbonation, the aluminum tapes on the surfaces of the samples were peeled off, then the surfaces were polished by sandpaper to remove the attached butyl from the surface. The specimens were divided into two groups. One group of the samples was cut along with the carbonation direction, and three sliced samples at each carbonation condition were used to measure the carbonation depth by 1% phenolphthalein solution. The other one was cut into five slices perpendicular to the carbonation direction (about 4 mm thick) which were quantified by X-ray diffraction (XRD) and Rietveld analysis.

2.3 Characterization of Materials

The two specimens under each carbonation condition at the determined carbonation duration (0, 1, 3, 7, 14, and 28 days) were taken out and placed inside the x-ray CT scanner (inspeXio SMX-100CT system, Shimadzu) as shown in Fig. 2. The moisture penetration depth was detected by X-ray computed radiography (CR) by taking the transmission images [9] where tube voltage of 100kV, the tube current of 65μA, the SDD (distance from the X-ray focus to the detector) of 500 mm, and the SRD (distance from the x-ray focus to the sample) of 350 mm were used. The number of feed lines was two, and the radiography was performed using a Cu filter with a thickness of 0.2 mm. The spatial resolution of the picture was 0.043mm/pixel. After each time of transmission imaging, the sample was put back into the carbonation incubator for the continuous carbonation process. The moisture penetration depth of the sample at each determined carbonation period can be visualized by subtracting the initial image right after the drying process (0 day) from the X-ray transmission images taken by using an open-source image analysis software Image J [10]. Since the electron density between solid and liquid detected by X-ray radiography is much larger than the solid phases before and after carbonation, the effect of the density change of the solid phase due to carbonation can be ignored.

In addition, the slices cut along the carbonation depth of the samples after 28 days' carbonation period were smashed by a hammer to pieces with a size under 5mm, and then vacuum-dried for 24h to stop carbonation. Then they were grounded by a hybrid mill (YOSHIDA SEISAKUSHO) to the powder with a size under 75μm, whose phase compositions were identified and quantified by XRD/Rietveld analysis, using a PANalytical Empyrean diffractometer with Cu kα radiation, using a 2θ can range of 5°-70° and a scan speed of 2°/min.

3. RESULTS AND DISCUSSION

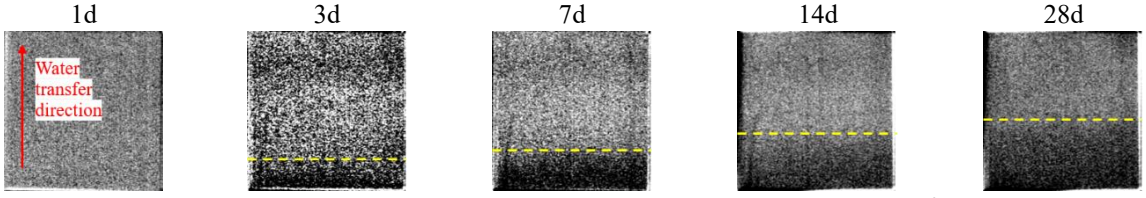

Fig. 3 Moisture penetration in cement paste at 58% RH and 20℃ (dashed line represents the moisture penetration depth)

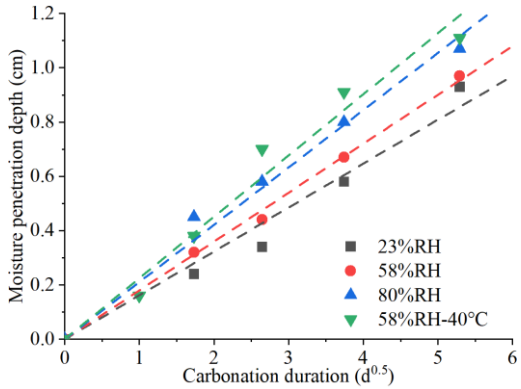

Fig.4 Moisture penetration depth with time under different carbonation conditions

3.1 Moisture penetration depth

Fig. 3 shows the representative visualization images of moisture distribution and penetration front in cement paste at 58% RH and 20℃ at 1, 3, 7, 14, and 28 days after processing the subtraction of images. The dark area represents the region in which the water was absorbed in the mortar specimen. The relationship between average pixel value and distance from water absorbed surface can be obtained from these figures. The moisture penetration depth can be determined from the position where the sharp change of pixel value appears [9]. The changes in moisture penetration depths of samples at each carbonation condition with the square root of carbonation period are summarized and fitted by linear lines passed through the origin of the coordinate in Fig. 4. Accordingly, the moisture penetration depth at 28 days and the penetration rate, which is the slope of fitting line, can be calculated and listed in Table 3. From these results, the moisture penetration depth and rate increase with the increasing RH until 80% at 20℃. The highest penetration depth and rate occur in the sample at 58% RH with 40℃. This indicates that the moisture movement was promoted by increasing RH and elevating temperature.

Table 3 Moisture penetration depth at 28 days and penetration rate

Carbonation conditions	Penetration depth at 28d (mm)	Penetration rate (mm/$\sqrt{t}$)
23%RH	9.3±0.1	0.16
58%RH	9.7±0.1	0.18
80%RH	10.7±0.2	0.21
58%RH-40℃	11.1±0.2	0.23

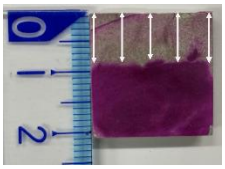

Fig. 5 Carbonation depth tested by phenolphthalein solution

Table 4 Carbonation depth in cement paste at 28 days

Carbonation conditions	Carbonation depth at 28d (mm)
23%RH	5.8±0.2
58%RH	8.8±0.1
80%RH	8.5±0.1
58%RH-40℃	9.3±0.1

3.2 Carbonation depth

The carbonation depth can be determined by measuring the length from the exposed surface to the closest boundary between the purple region and the gray region at fix points carried out by phenolphthalein test on the cross-sectional area of samples[11], as shown in Fig. 5. Table 4 shows the carbonation depth results, which were carbonated under different conditions for 28 days. It can be observed that at the same temperature condition of 20℃, the maximum carbonation depth (8.8 mm) occurs at the RH of 58%, which proved that moderate RH is the optimal condition for carbonation. This result is consistent with the conclusions in [5][12]. Previous research [13] stated that the carbonation process needs a sufficient thick and continuous water film on the CH crystal surface, which is difficult to be established in the dry condition (23%RH), while can be realized at moderate and high humidity conditions (58% and 80%RH). However, at the high RH condition, pore blockage by water tends to inhibit CO_2 ingress, which limits the growth of the carbonation front [14].

Besides, given the same RH condition of 58%, the carbonation depth detected at 40℃ is higher than 20℃. This was because the transmission coefficient of CO_2 and the chemical reaction coefficient was accelerated by elevating temperature[7].

3.3 Mineralogical profile and carbonation degree

Fig. 6 shows the mineralogical profiles quantified by Rietveld analysis from XRD results along the carbonation depth under each environmental condition after carbonated for 28 days. In general, the calcium carbonate (calcite, vaterite, aragonite) decreases, while the portlandite increases with increasing depth. In all cases, the CH remained at each slice in the carbonated zone. It is related to the formation of calcium carbonate crystals coated around CH crystals, which inhibits the ion availability and slows down the further dissolution of CH [15]. For the calcium carbonate phases, calcite is the predominant phase of carbonation products at 58% and 80% RH conditions, but it no longer the major phase of calcium carbonate at 23% RH condition, where the predominant phase is aragonite. The highest calcite content existed at the carbonated zone of cement paste at 80% RH, which is attributed to the transformation from aragonite and vaterite to calcite where the moisture is sufficient, but such phase change will be inhibited when moisture is low [16].

Furthermore, it is interesting to notice that the position of the highest calcite content occurred along the carbonation direction tend to be consistent with the carbonation front detected by the phenolphthalein solution denoted by the red dashed lines in Fig. 6, especially at the 58%RH and 80%RH conditions. This could be supposed that the carbonizing substances (Ca^{2+}, HCO_3^-, CO_3^{2-}) may move together with the moisture distribution, and covert to the stable phase (calcite) with time, which need to be verified further.

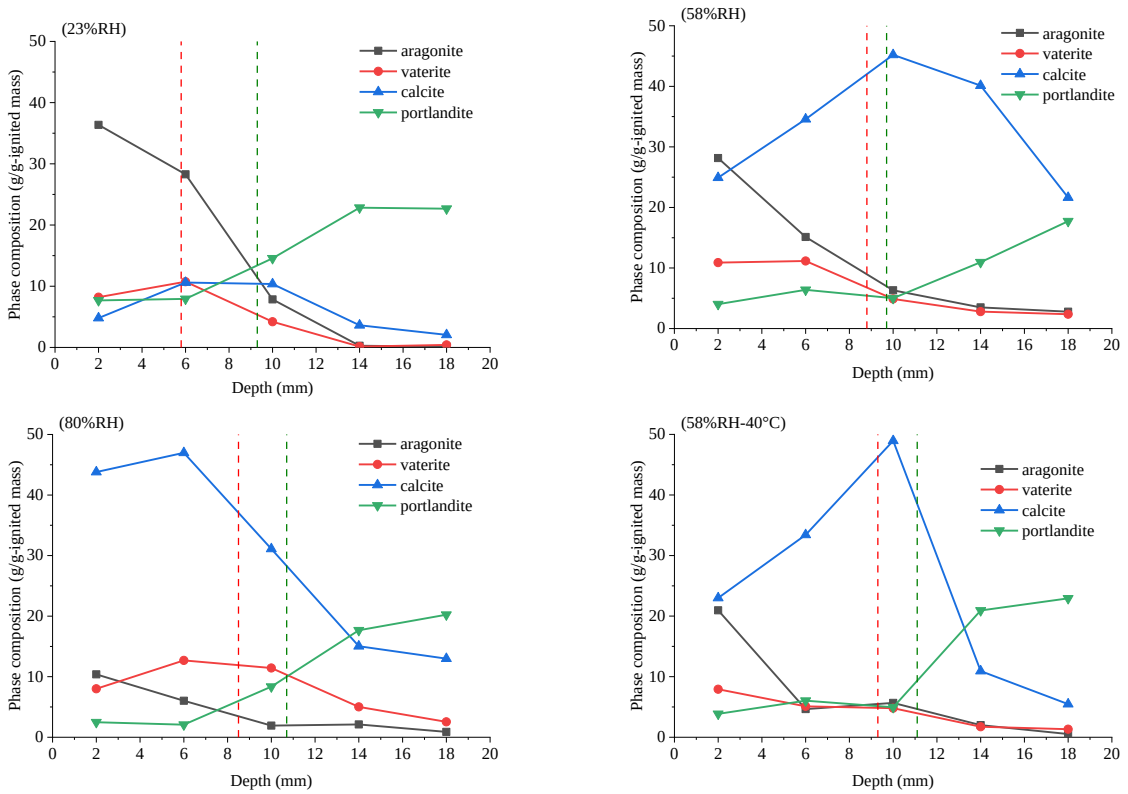

Fig. 6 Mineralogical profile of carbonated samples at different carbonation conditions (red dashed line denotes the carbonation front tested by phenolpohetahlei solution, green dashed line denotes the moisture penetration front tested by CR images)

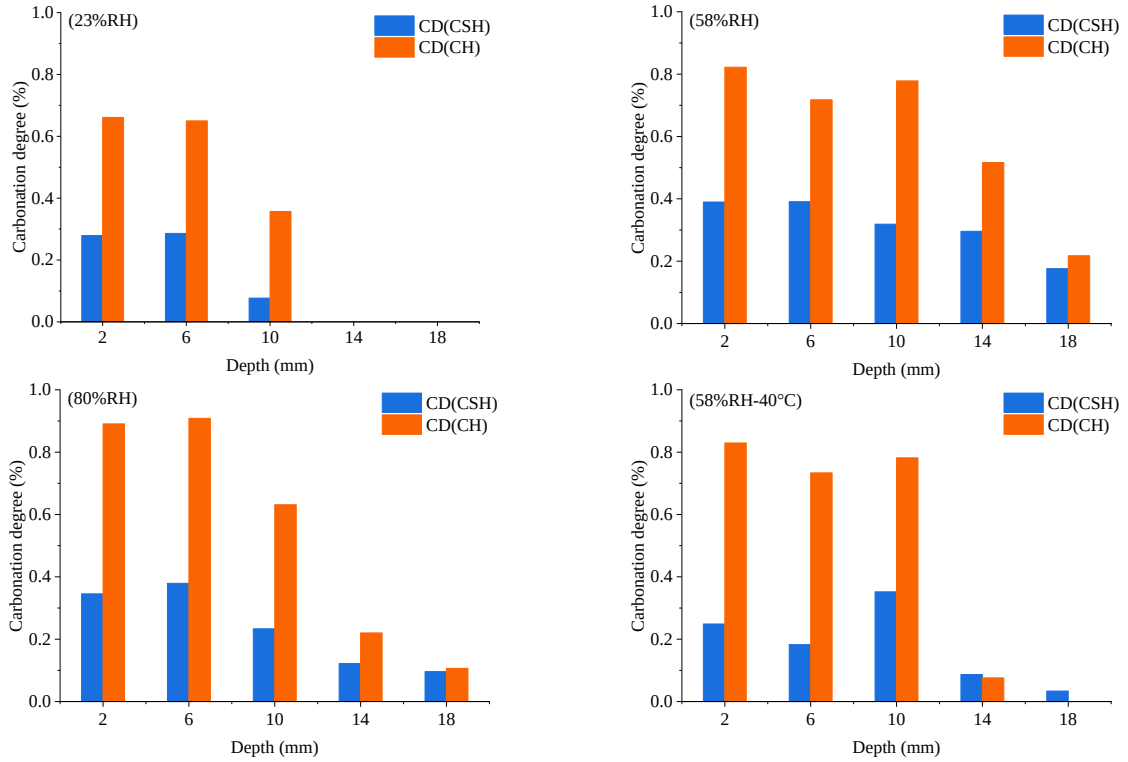

Fig. 7 carbonation degrees of CH and C-S-H of carbonated samples at different carbonation conditions

To correlate the moisture penetration with the amount of calcium carbonate related to CH and C-S-H carbonation (neglect the carbonation of ettringite due to the minor content), the amount of carbonation degree of CH (CD_{CH}) and C-S-H (CD_{CSH}) were calculated as below:

$$CD_{CH} = (m_{CH}^0 - m_{CH})/m_{CH}^0 \quad (1)$$

$$CD_{CSH} = (m_{CC} - \frac{m_{CH}^0 - m_{CH}}{M_{CH}} \cdot M_{CC} - m_{CC}^0)/(1.83M_{CC} \cdot \frac{m_{CSH}^0}{162.48}) \quad (2)$$

where, m_{CH}^0, m_{CC}^0 and m_{CSH}^0 are the initial content of CH, CC, and C-S-H (amorphous content) of the cement paste before carbonation quantified by XRD/Rietveld

analysis, respectively. m_{CC} and m_{CH} are the content of CC and CH at each slice determined carbonation period. M_{CH} and M_{CC} are the molar mass of CH and CC, which are 74g/mol and 100g/mol, respectively. The C/S ratio of C-S-H was obtained following the method in [17], which was calculated as 1.83 in this study, and 162.48 is the molar mass of $(CaO)_{1.83}(SiO_2)$. Since all the mineral contents were calculated as the ratio of ignited cement paste, the content of water in C-S-H was not considered in this study.

The results of the carbonation degrees of CH and C-S-H in samples under different carbonation conditions are shown in Fig. 7. The carbonation degrees of CH and C-S-H decrease along the carbonation direction under all the carbonation conditions, and show a dramatic drop near the carbonation front (Fig. 6). Since the color change of phenolphthalein solution is related to the remained content of CH [18], in this study, the position of color change boundary varied depending on different CD_{CH} under four carbonation conditions. The purple color appears in the following situations: remained ratio of CH ($R_{CH} = 1 - CD_{CH}$) is higher than 34% at 23% RH condition, R_{CH} is higher than 23% at 58%RH condition, R_{CH} is higher than 10% at 80% RH condition, and R_{CH} is higher than 22% at 58%RH and 40℃ condition. It shows that the color appeared area by phenolphthalein indicator tends to be wider under higher RH conditions due to the higher water content of sample. When the RH is low, the dissolved CH is also low due to the low water content, which makes the indication of phenolphthalein solution for alkali conditions difficult. When the RH becomes higher, the CH can be dissolved in sufficient water even if the amount of CH is low, which promotes the indication of phenolphthalein solution for alkali conditions

At the carbonated zone (the left side from the red lines in Fig. 6), the average of CD_{CSH} shows the highest value at 58% RH and 20℃, while the lowest value at 58%RH and 40℃, although oscillates in a narrow range of 0.26 to 0.36 regardless of carbonation conditions. On the other hand, it is obvious that CD_{CH} increases from 0.63 to 0.90 when the RH increases from 23% to 80% at 20℃, which is supported by the reduction of remaining CH content at the carbonated zone when RH increases in Fig. 6. The behavior that the CD_{CH} at high RH (higher than 80%) tends to be higher has also been reported in [13] [19]. This behavior also can be attributed to the thicker water film consisting of a higher number of water monolayers at higher RH conditions, which allows the calcium carbonate to nucleate in the aqueous layer and the crystal/solution interface [15]. Therefore, the inhibiting effect of CC for the dissolution of CH is little at 80% RH, which leads to the highest carbonation degree of CH.

3.4 Comparison between carbonation depth and moisture penetration depth

The effect of carbonation on moisture penetration can be evaluated by two aspects: pore-clogging and microcracking. Precipitation of calcium carbonate formed by carbonation reaction generates pore-clogging, which is responsible for the reduction of water permeability, while the microcracking due to carbonation shrinkage of C-S-H was believed to be the major cause of the water permeability increase. The effect of such two controversial effects of water permeability can be differentiated by observing the distance between the carbonation depth and moisture penetration depth.

The carbonation depth detected by the phenolphthalein solution and moisture penetration depth obtained by CR images are marked by red and green dashed lines, respectively in Fig. 6. Since the liquid water is necessary for the carbonation reaction, therefore, the carbonation depth is always behind moisture penetration depth. It clearly shows that the distance between the moisture penetration depth and carbonation depth ranges from 0.9 to 3.5 mm. At 23% RH, the distance between the carbonation depth and the moisture penetration depth is the largest (Fig. 6), which indicates that the effect of microcracking formed by decalcification of C-S-H on moisture penetration is predominant, which was supported by the mineralogical profiles at the carbonated zone (Fig. 6) and the carbonation degrees of C-S-H and CH (Fig. 7). The carbonation degree of CH (0.65) at 23% RH condition is much lower than the other carbonation conditions, while the carbonation degree of C-S-H is around 0.28, which is at a similar level in other cases. This phenomenon indicates that the extent of the microcracking effect is relatively greater than in other conditions. On the other hand, since the density of aragonite (2.93g/cm^3) is higher than calcite (2.71g/cm^3), the predominated CC of aragonite with the lowest expansion volume reduces the pore-clogging effect. Therefore, the microcracking effect on moisture penetration prevailed over the pore-clogging effect, leading to much faster moisture penetration than the carbonation depth under 23% RH.

On the contrary, the carbonation depth and moisture penetration depth are similar at the conditions of 58% RH and 20℃ (Fig. 6). This fact was related to the relatively high content of calcite and high carbonation degree of CH (Fig. 7), which indicates the effect of pore-clogging on water permeability was counterbalanced by microcracking.

In the condition of 80% RH, the higher water content among pores inhibits CO_2 transfer even though the calcite content and carbonation degree of CH at the carbonated zone are the highest (Fig. 6 and Fig. 7). Therefore, the limited carbonation leads to the relatively larger distance between carbonation depth and moisture penetration depth, although the water permeability through the carbonated area may decreases by the pore-clogging.

For the effect of temperature on carbonation and moisture penetration, elevating temperature accelerates both the carbonation process and moisture penetration. Besides, it can be observed that the distance between the carbonation depth and moisture penetration depth at 58% RH and 40℃ condition is larger than that at 58% RH and 20℃ condition. Given the same RH condition, the promotion effect of increasing temperature on moisture penetration is more significant than on the carbonation process.

3. CONCLUSIONS

According to the carbonation depth and moisture penetration depth in cement paste, with the characterized three crystalline polymorphs of carbonation products distribution and carbonation degree of CH and C-S-H along the carbonation direction, the effect of RH and temperature on moisture penetration and carbonation behavior was clarified:

1) The increasing RH leads to the increase of carbonation degree of CH while inhibiting the CO_2 ingress by water blockage, the optimum RH for carbonation was found to be 58% in the experiment.

2) The predominant phase is calcite when RH is above 58%, while aragonite is the predominant one when RH is 23% because the transformation from aragonite and vaterite to calcite was inhibited due to the lack of water.

3) Increasing temperature was found to promote both the carbonation process and moisture penetration. The promotion effect of increasing temperature on moisture penetration is more significant than the carbonation process.

The opposite effects of carbonation on moisture penetration properties through the cement paste can also be interpreted:

1) The microcracking effect on water permeability prevailed over the pore-clogging effect at 23% RH, which was illustrated from the largest distance between moisture penetration depth and carbonation depth, due to the predominate phase of aragonite with a higher density, and the lowest carbonation degree of CH at carbonated zone.

2) The effect of pore-clogging on water permeability was counterbalanced by microcracking at 58% RH and 20℃, which was interpreted from the similar depth of moisture penetration and carbonation, attributed to the higher carbonation reaction of CH and calcite content.

ACKNOWLEDGEMENT

This study was supported by the Green Innovation Fund Project of the New Energy and Industrial Technology Development Organization (NEDO), "Research and Development on Standardization of Evaluation of CO_2 Fixation in Concrete," led by Professor Ippei Maruyama (The University of Tokyo).

REFERENCES

[1] E. Dubina, L. Korat, L. Black, J. Strupi-Šuput, and J. Plank, “Influence of water vapour and carbon dioxide on free lime during storage at 80°C, studied by Raman spectroscopy,” *Spectrochim. Acta - Part A Mol. Biomol. Spectrosc.*, vol. 111, pp. 299–303, 2013.

[2] V.T.Ngala and C.L.Page, “Effects of Carbonation on Pore Structure and Diffusional Properties of Hydrated Cement Pastes,” *Cem. Concr. Res.*, vol. 27, no. 7, pp. 995–1007, 1997.

[3] P. Van Den Heede, M. De Schepper, and N. De Belie, “Accelerated and natural carbonation of concrete with high volumes of fly ash: Chemical, mineralogical and microstructural effects,” *R. Soc. Open Sci.*, vol. 6, no. 1, pp. 1–19, 2019.

[4] I. Galan, C. Andrade, and M. Castellote, “Natural and accelerated CO_2 binding kinetics in cement paste at different relative humidities,” *Cem. Concr. Res.*, vol. 49, pp. 21–28, 2013.

[5] X. Fang, D. Xuan, and C. S. Poon, “Empirical modelling of CO_2 uptake by recycled concrete aggregates under accelerated carbonation conditions,” *Mater. Struct. Constr.*, vol. 50, no. 4, pp. 1–13, 2017.

[6] D. Wang, T. Noguchi, and T. Nozaki, “Increasing efficiency of carbon dioxide sequestration through high temperature carbonation of cement-based materials,” *J. Clean. Prod.*, vol. 238, p. 117980, 2019.

[7] E. Drouet, S. Poyet, P. Le Bescop, J. M. Torrenti, and X. Bourbon, “Carbonation of hardened cement pastes: Influence of temperature,” *Cem. Concr. Res.*, vol. 115, no. September 2018, pp. 445–459, 2019.

[8] Y. Chen, P. Liu, and Z. Yu, “Effects of environmental factors on concrete carbonation depth and compressive strength,” *Materials (Basel).*, vol. 11, no. 11, pp. 1–11, 2018.

[9] S. Roels and J. Carmeliet, “Analysis of moisture flow in porous materials using microfocus X-ray radiography,” *Int. J. Heat Mass Transf.*, vol. 49, no. 25–26, pp. 4762–4772, 2006.

[10] C. A. Schneider, W. S. Rasband, and K. W. Eliceiri, “NIH Image to ImageJ: 25 years of image analysis,” *Nat. Methods*, vol. 9, no. 7, pp. 671–675, 2012.

[11] *JIS A 1152 Method for measuring carbonation depth of concrete*. JCI.

[12] G. Li, Y. S. Yuan, X. Liu, J. M. Du, and F. M. Li, “Influences of environment climate conditions on concrete carbonation rate,” *Adv. Mater. Res.*, vol. 194–196, pp. 904–908, 2011.

[13] S. M. Shih, C. S. Ho, Y. S. Song, and J. P. Lin, “Kinetics of the reaction of $Ca(OH)_2$ with CO_2 at low temperature,” *Ind. Eng. Chem. Res.*, vol. 38, no. 4, pp. 1316–1322, 1999.

[14] M. Elsalamawy, A. R. Mohamed, and E. M. Kamal, “The role of relative humidity and cement type on carbonation resistance of concrete,” *Alexandria Eng. J.*, vol. 58, no. 4, pp. 1257–1264, 2019.

[15] I. Galan, F. P. Glasser, D. Baza, and C. Andrade, “Assessment of the protective effect of carbonation on portlandite crystals,” *Cem. Concr. Res.*, vol. 74, pp. 68–77, 2015.

[16] I. Maruyama *et al.*, “Impact of gamma-ray irradiation on hardened white Portland cement pastes exposed to atmosphere,” *Cem. Concr. Res.*, vol. 108, no. March, pp. 59–71, 2018.

[17] N. Koga, K. Tsuru, I. Takahashi, and K. Ishikawa, “Effects of humidity on calcite block fabrication using calcium hydroxide compact,” *Ceram. Int.*, vol. 41, no. 8, pp. 9482–9487, 2015.

[18] 岸谷孝一, “コンクリート中の鉄筋の腐食に関する基礎的研究ー中性化とフェノールフタレイン,” *Archit. Inst. Japan*, pp. 95–96, 1969.

[19] M. Zajac, J. Skibsted, F. Bullerjahn, and J. Skocek, “Semi-dry carbonation of recycled concrete paste,” *J. CO_2 Util.*, vol. 63, no. April, pp. 1–17, 2022.